Photoluminescence and Terahertz Emission from Femtosecond Laser-Induced Plasma Channels

W. Hoyer,* A. Knorr,† J. V. Moloney, and E. M. Wright
Arizona Center for Mathematical Sciences and Optical Sciences Center, University of Arizona, Tucson, Arizona 85721, USA

M. Kira and S. W. Koch
Department of Physics and Material Sciences Center, Philipps-University, Renthof 5, D-35032 Marburg, Germany
(Received 3 September 2004; published 24 March 2005)

Luminescence as a mechanism for terahertz emission from femtosecond laser-induced plasmas is studied. By using a fully microscopic theory, Coulomb scattering between electrons and ions is shown to lead to luminescence even for a spatially homogeneous plasma. The spectral features introduced by the rod geometry of laser-induced plasma channels in air are discussed on the basis of a generalized mode-function analysis.

DOI: 10.1103/PhysRevLett.94.115004 PACS numbers: 52.20.–j, 52.25.Os

The past decade has seen increasing activity in the generation and detection of far-infrared or terahertz (THz) radiation with an accompanying increase in applications, including time-domain THz spectroscopy and THz tomography [1]. Current THz sources have a limited spatial extent (μm to mm), such as transient antenna emitters, sources based on optical rectification, and quantum cascade lasers. A notable exception is the observation of THz radiation emitted from plasma channels induced in air by femtosecond (fs) infrared filaments [2–4], or light strings, that can extend over centimeters [5–8]. The extension of these results to other media offers the possibility of a new variety of extended THz sources.

In addition to the technological importance of light strings for realizing THz sources, the mechanism of THz emission raises basic physics issues. To date most theory and experiments on *coherent* THz emission in air have considered localized plasmas with volumes $\simeq \mu\mathrm{m}^3$ [9], much less than λ_{THz}^3 for typical THz wavelengths. In contrast, light string induced plasmas can be significantly longer than λ_{THz} along the propagation direction of the exciting laser meaning that coherent emissions from different locations in the plasma need not add constructively [10]. In this Letter, we propose *incoherent* light emission by a two-component plasma as a viable mechanism for THz emission since this does not rely on the establishment of relative phases between emissions from different locations in the plasma. We develop a microscopic theory which includes the Coulomb interaction between the charge carriers and the light-matter interaction with a quantized light field. First, we calculate the broadband radiation of a homogeneous plasma due to electron-ion scattering. Second, we make a mode-function analysis for the specific rodlike geometry for light string induced plasmas in air in order to explore the angular dependence of the THz emission. The luminescence mechanism itself is similar to what is commonly referred to as bremsstrahlung. Many of the previous results, however, were obtained indirectly from collisional absorption using Kirchhoff's law, which requires complete thermal equilibrium [11–13], or under the assumption of a homogeneous plasma [14,15]. In contrast, our approach is ideally suited to deal with the realistic geometry of the emitting system.

Our starting point is the total Hamiltonian

$$H_{\mathrm{tot}} = \sum_{\lambda} (H_{\mathrm{kin}}^{\lambda} + H_{A\cdot p}^{\lambda} + H_{A^2}^{\lambda}) + H_{\mathrm{L}} + H_{\mathrm{C}}, \qquad (1)$$

where $\lambda = e, i$ sums over electron and ion contributions. It arises from the minimal coupling Hamiltonian $H_{\mathrm{min}}^{\lambda} = \int d^3 r \Psi_{\lambda}^{\dagger}(\mathbf{r}) \frac{[\hat{\mathbf{p}} - q_{\lambda}\mathbf{A}(\mathbf{r})]^2}{2m_{\lambda}} \Psi_{\lambda}(\mathbf{r})$ applied to our system [16], where $\Psi_{\lambda}(\mathbf{r})$ and $\Psi_{\lambda}^{\dagger}(\mathbf{r})$ are the annihilation and creation operators for electrons and ions, respectively, m_{λ} and q_{λ} are the particle masses and charges, $\mathbf{A}(\mathbf{r}) = \sum_{\mathbf{q},\sigma} (\mathcal{A}_q B_{\mathbf{q},\sigma} e^{i\mathbf{q}\cdot\mathbf{r}} \boldsymbol{\epsilon}_{\mathbf{q},\sigma} + \mathrm{H.c.})$ is the quantized vector potential operator. Here $\mathcal{A}_q = \sqrt{\hbar/(2\varepsilon_0 \omega_q V)}$, and we introduced the boson operators $B_{\mathbf{q},\sigma}(B_{\mathbf{q},\sigma}^{\dagger})$ which annihilate (create) photons with wave number $\mathbf{q}$ and polarization direction $\boldsymbol{\epsilon}_{\mathbf{q},\sigma}$, in terms of which the free-field Hamiltonian appearing in Eq. (1) is $H_{\mathrm{L}} = \sum_{\mathbf{q},\sigma} \hbar\omega_q (B_{\mathbf{q},\sigma}^{\dagger} B_{\mathbf{q},\sigma} + \frac{1}{2})$. We work in the $\mathbf{A}\cdot\mathbf{p}$ picture and formulate our equations in momentum space, the relation between real and momentum space operators being $\Psi_{\lambda}(\mathbf{r}) = 1/\sqrt{V}\sum_{\mathbf{k}} e^{i\mathbf{k}\cdot\mathbf{r}} a_{\lambda,\mathbf{k}}$, where the operator $a_{\lambda,\mathbf{k}}$ annihilates a particle of species λ with momentum $\hbar\mathbf{k}$. The kinetic energy term in the Hamiltonian (1) is then given by $H_{\mathrm{kin}}^{\lambda} = \sum_{\mathbf{k}} \varepsilon_k^{\lambda} a_{\lambda,\mathbf{k}}^{\dagger} a_{\lambda,\mathbf{k}}$, with free-particle energies $\varepsilon_k^{\lambda} = \hbar^2 k^2/(2m_{\lambda})$, and the light-matter interaction terms become

$$H_{A\cdot p}^{\lambda} = -\sum_{\mathbf{k},\mathbf{q}} \mathbf{J}_{\mathbf{k}}^{\lambda} \cdot \mathbf{A}_{\mathbf{q}} a_{\lambda,\mathbf{k}+\mathbf{q}/2}^{\dagger} a_{\lambda,\mathbf{k}-\mathbf{q}/2}, \qquad (2)$$

with the canonical current matrix element $\mathbf{J}_{\mathbf{k}}^{\lambda} = q_{\lambda}\hbar\mathbf{k}/m_{\lambda}$, and the Fourier transformed operator of the vector potential $\mathbf{A}_{\mathbf{q}}$, along with the nonlinear A^2 contribution

$$H_{A^2}^{\lambda} = \frac{q_{\lambda}^2}{2m_{\lambda}} \sum_{\mathbf{k},\mathbf{q},\mathbf{q}',s} \mathbf{A}_{\mathbf{q}'}^{\dagger} \cdot \mathbf{A}_{\mathbf{q}} a_{\lambda,\mathbf{k}+\mathbf{q},s}^{\dagger} a_{\lambda,\mathbf{k}+\mathbf{q}',s}. \qquad (3)$$

Finally, Coulomb interactions between charges are incorporated in the total Hamiltonian (1) using

$$H_{\mathrm{C}} = \frac{1}{2} \sum_{\substack{\lambda,\lambda' \\ \mathbf{k},\mathbf{k}',\mathbf{q}}} V_q^{\lambda,\lambda'} a^\dagger_{\lambda,\mathbf{k}} a^\dagger_{\lambda',\mathbf{k}'} a_{\lambda',\mathbf{k}'+\mathbf{q}} a_{\lambda,\mathbf{k}-\mathbf{q}} \tag{4}$$

with the Coulomb matrix element $V_q^{\lambda,\lambda'}$ [17].

We work in the Heisenberg picture where the quantum average of an operator O evolves according to $i\hbar\partial\langle O\rangle/\partial t = \langle[O, H_{\mathrm{tot}}]\rangle$. Here, the many-body Coulomb and the light-matter interaction introduce a hierarchy problem such that, e.g., photon numbers $\langle B^\dagger B\rangle$ are coupled to mixed correlations of $\langle B^\dagger a^\dagger a\rangle$ which in turn become coupled to higher-order expectation values. We truncate this hierarchy using a cluster expansion [18,19] where multiparticle or mixed expectation values are consistently factorized. For example, photon correlation functions are split according to

$$\langle B^\dagger_{\mathbf{q}',\sigma'} B_{\mathbf{q},\sigma}\rangle = \langle B^\dagger_{\mathbf{q}',\sigma'}\rangle\langle B_{\mathbf{q},\sigma}\rangle + \Delta\langle B^\dagger_{\mathbf{q}',\sigma'} B_{\mathbf{q},\sigma}\rangle, \tag{5}$$

with $\langle B_{\mathbf{q},\sigma}\rangle$ related to the coherent component of the field and $\Delta\langle B^\dagger_{\mathbf{q}',\sigma'} B_{\mathbf{q},\sigma}\rangle$ describing quantum fluctuations.

Here we are interested in incoherent light emission under quasistationary conditions after the exciting laser has passed, and an appropriate measure of the photoluminescence is the total rate of energy emitted into a single mode $(\mathbf{q}, \sigma)$ given by

$$I^{\mathrm{PL}}_{\mathbf{q},\sigma} = \hbar\omega_q \frac{\partial}{\partial t}\langle B^\dagger_{\mathbf{q},\sigma} B_{\mathbf{q},\sigma}\rangle = \hbar\omega_q \frac{\partial}{\partial t}\Delta\langle B^\dagger_{\mathbf{q},\sigma} B_{\mathbf{q},\sigma}\rangle, \tag{6}$$

where we have neglected any coherent field contribution. The Heisenberg equation of motion for the photon number is found to be

$$\frac{\partial}{\partial t}\Delta\langle B^\dagger_{\mathbf{q},\sigma} B_{\mathbf{q},\sigma}\rangle = -\frac{2}{\hbar}\,\mathrm{Im}\Big[\sum_{\mathbf{k}} \mathbf{J}^e_{\mathbf{k}} \cdot \boldsymbol{\epsilon}^*_{\mathbf{q},\sigma} \mathcal{A}_q \times \Delta\langle B^\dagger_{\mathbf{q},\sigma} e^\dagger_{\mathbf{k}-\mathbf{q}/2} e_{\mathbf{k}+\mathbf{q}/2}\rangle\Big], \tag{7}$$

where we have defined $e_{\mathbf{k}} \equiv a_{\lambda=e,\mathbf{k}}$ for notational simplicity. Here we have neglected the A^2 contribution in order to investigate the general emission mechanism. We show later that its influence can be accounted for by generalized mode functions of the quantized field such that all our calculations remain valid. From Eq. (7) we see that the incoherent emission of photons is driven by photon-assisted densities of the form $\Delta\langle B^\dagger_{\mathbf{q},\sigma} e^\dagger_{\mathbf{k}-\mathbf{q}/2} e_{\mathbf{k}+\mathbf{q}/2}\rangle$, which correspond to processes where an electron changes its momentum, while emitting a photon with the corresponding momentum difference. Under the assumption of large ion masses we have neglected a similar contribution from photon-assisted ion densities $\Delta\langle B^\dagger p^\dagger p\rangle$. To evaluate the dynamics of $\Delta\langle B^\dagger_{\mathbf{q},\sigma} e^\dagger_{\mathbf{k}-\mathbf{q}/2} e_{\mathbf{k}+\mathbf{q}/2}\rangle$ we apply the long wavelength and low density limit; the procedure leads to

$$i\hbar\frac{\partial}{\partial t}\Delta\langle B^\dagger_{\mathbf{q},\sigma} e^\dagger_{\mathbf{k}-\mathbf{q}/2} e_{\mathbf{k}+\mathbf{q}/2}\rangle = \Big(\frac{\hbar^2(\mathbf{k}\cdot\mathbf{q})}{m_e} - \hbar\omega_q - i\Gamma^D_{\mathbf{k}}(q)\Big)\Delta\langle B^\dagger_{\mathbf{q},\sigma} e^\dagger_{\mathbf{k}-\mathbf{q}/2} e_{\mathbf{k}+\mathbf{q}/2}\rangle + i\sum_{\mathbf{k}'}\Gamma^{OD}_{\mathbf{k},\mathbf{k}'}(q)\Delta\langle B^\dagger_{\mathbf{q},\sigma} e^\dagger_{\mathbf{k}'-\mathbf{q}/2} e_{\mathbf{k}'+\mathbf{q}/2}\rangle + \mathcal{A}_q \boldsymbol{\epsilon}_{\mathbf{q},\sigma}\cdot\mathbf{J}^e_{\mathbf{k}} f^e_{\mathbf{k}}, \tag{8}$$

where the last term corresponds to the spontaneous emission source term.

It is well known that a single-component, noninteracting plasma cannot emit or absorb radiation while simultaneously conserving energy and momentum. However, in Coulomb interacting systems such restrictions do not apply. In the following, we concentrate on the scattering between electrons and ions, symbolized by Γ^D and Γ^{OD} in Eq. (8). We numerically confirmed that emission due to electron-electron scattering is negligible compared to the electron-ion scattering. Additional mechanisms such as electron-neutral scattering will increase the scattering rates but are not expected to change the qualitative picture. A microscopic description of the scattering is obtained by including the coupling of the photon-assisted densities to photon-assisted correlations of the form $\Delta\langle B^\dagger e^\dagger p^\dagger p e\rangle$, deriving the Heisenberg equation of motion for this quantity, and factorizing the resulting higher-order correlations in products of the form $f(1-f)\Delta\langle B^\dagger e^\dagger e\rangle$. By Fourier transformation this equation can be formally solved and inserted into Eq. (8) in the form of frequency-dependent scattering matrices

$$\Gamma^{OD}_{\mathbf{k},\mathbf{k}'}(q) = \frac{(-i)W^2_{|\mathbf{k}-\mathbf{k}'|}\sum_{\mathbf{k}''} f^i_{\mathbf{k}''}}{\varepsilon^e_{\mathbf{k}'} - \varepsilon^e_{\mathbf{k}} - \hbar\omega_q - i\delta} + \{\omega_q \leftrightarrow -\omega_q\}^*, \tag{9}$$

with diagonal elements $\Gamma^D_{\mathbf{k}}(q) = \sum_{\mathbf{k}'}\Gamma^{OD}_{\mathbf{k}',\mathbf{k}}(q)$, where $W_{|\mathbf{k}-\mathbf{k}'|}$ denotes the statically screened Coulomb matrix element [17] and large ion mass and low density limit are applied. The frequency dependence of the scattering derives from the presence of the photon operator in the photon-assisted correlations. Inspection of the denominator in Eq. (9) shows that an electron changes momentum due to Coulomb interaction with an ion. The corresponding change in kinetic energy is accounted for by photon emission while the total change of momentum of the electron is absorbed by the heavy ions.

Figure 1 shows the calculated $I^{\mathrm{PL}}_{\mathbf{q},\sigma}$ as function of frequency for a homogeneous plasma with different electron densities and temperatures. The temperatures lie in the

range of typical excess energies of about 0.25 eV for multiphoton ionization. We observe that the spectra are sharply peaked around $\omega = 0$. The emission at $\omega = 0$ is mainly determined by the plasma temperature while the width of the emission tail increases with elevated density. In order to understand these results, we approximate the microscopic (k-dependent) scattering matrices by an effective constant damping rate γ_{eff}. In that case, Eq. (8) can be formally solved and inserted into Eq. (7), which upon assuming Maxwell-Boltzmann distributions for the electrons and taking the low density limit yields

$$I^{\text{PL}}_{\mathbf{q},\sigma} = \omega_{\text{pl}}^2 k_{\text{B}} T \frac{\gamma_{\text{eff}}}{\omega_q^2 + \gamma_{\text{eff}}^2}. \tag{10}$$

Here γ_{eff} plays the role of an electron-ion collision frequency [15]. Assuming a linear dependence of γ_{eff} on density in agreement with Eq. (9), we find that the high-frequency luminescence is proportional to $\omega_{\text{pl}}^2 \gamma_{\text{eff}} \propto n^2$ while the low-frequency behavior is determined by $\omega_{\text{pl}}^2/\gamma_{\text{eff}} \propto 1$ and thus is independent of density. For low frequencies, Fig. 1 also exhibits the trend of decreasing emission strength with decreasing temperature. The observed insensitivity of the high-frequency spectrum on temperature, however, cannot be explained with Eq. (10). Nevertheless, this equation can be used to fit an estimate for typical scattering times. For the case of $n = 10^{16}$ cm^{-3} and $T = 3000$ K we obtain a scattering time of the order of 2.5 ps.

Another shortcoming of Eq. (10) lies in the fact that for high frequencies it is proportional to $1/\omega^2$ such that the total power obtained as integral over $\mathcal{P}(\omega_q) = \omega_q^2 (2\pi^2 c^3)^{-1} I^{\text{PL}}_{\mathbf{q},\sigma}$ becomes divergent. In contrast, the microscopic, frequency-dependent scattering leads to an exponential decay as shown in the inset of Fig. 1. In order to obtain an estimate for the conversion efficiency of emission into the THz regime, we integrate $\mathcal{P}(\omega)$ from $\omega = 0$ up to $\omega = 50$ THz and obtain a value of roughly $\mathcal{P}_{\text{THz}} \approx 5 \times 10^4$ W/m^3. Comparing the total energy emitted by a plasma channel of radius $R = 30$ μm and length of $l = 1$ m over the characteristic lifetime $\tau = 1$ ns, $E = \pi R^2 l \tau \mathcal{P}_{\text{THz}} \approx 1.4 \times 10^{-13}$ J, with typical light string excitation energies in the range of 10 mJ, we obtain a conversion efficiency of $\eta \approx 1.4 \times 10^{-11}$ comparable to estimates for coherent emission mechanisms [10].

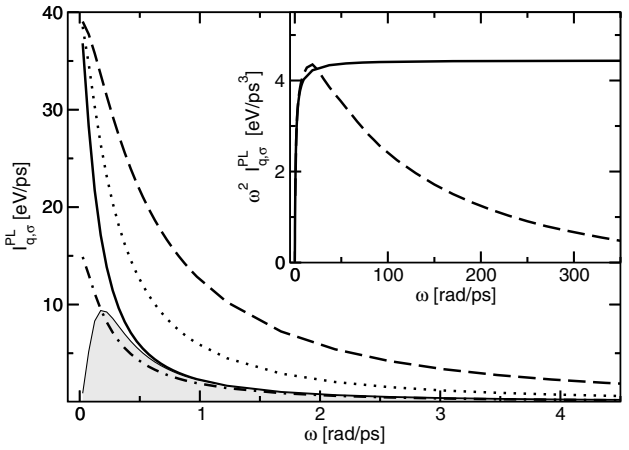

FIG. 1. Luminescence signal $I^{\text{PL}}_{\mathbf{q},\sigma}$ as a function of $\omega_q = cq$ for a plasma of density $n = 10^{16}$ cm^{-3} (solid line), $n = 2 \times 10^{16}$ cm^{-3} (dotted line), and $n = 4 \times 10^{16}$ cm^{-3} (dashed line) at $T = 3000$ K, and for $n = 10^{16}$ cm^{-3} at $T = 2000$ K (dash-dotted line). The shaded area is obtained by multiplication of the solid line with the mode strength $|\mathbf{u}_{\mathbf{q}}|^2$. Inset: data for $n = 10^{16}$ cm^{-3} and $T = 3000$ K after multiplication with ω^2 without (solid line) and with (dashed line) frequency-dependent scattering.

So far, we have completely neglected the influence of the A^2 contribution to the Hamiltonian. Instead of including the resulting terms into the equations of motion, we pursue a different approach. We approximate the density operator in Eq. (3) by its factorized expectation and assume that the overall density profile can be taken as time independent. In that case, $H^e_{A^2}$ is quadratic in the field in analogy to H_{L}. The combined $H^e_{A^2} + H_{\text{L}}$ can be diagonalized by choosing the light modes according to the generalized Helmholtz equation

$$c^2 \nabla \times \nabla \times \mathbf{u}_{\mathbf{q},\sigma}(\mathbf{r}) + \omega_{\text{pl}}^2(\mathbf{r}) \mathbf{u}_{\mathbf{q},\sigma}(\mathbf{r}) = \omega^2 \mathbf{u}_{\mathbf{q},\sigma}(\mathbf{r}) \tag{11}$$

with the space-dependent plasma frequency $\omega_{\text{pl}}(\mathbf{r}) = \sqrt{e^2 n(\mathbf{r})/(\varepsilon_0 m_e)}$. The computation of the new mode functions is a purely classical problem, the quantum character of the light field being fully contained in the photon operators. If the extension of the plasma is much larger compared to characteristic electronic length scales, the charge carriers still see an approximately three-dimensional environment. In that case, our previously calculated spectra have only to be multiplied by a frequency-dependent mode function. For a thin slab of constant density with a thickness d well below typical emission wavelengths, this prefactor for emission perpendicular to the plane of the plasma is given by

$$|\mathbf{u}_q(\mathbf{r} = 0)|^2 = \left(1 + \frac{1}{4} \frac{\omega_{\text{pl}}^4 d^2}{q^2 c^4}\right)^{-1}.$$

Thus, frequencies well below the plasma frequency are effectively suppressed. The shaded area in Fig. 1 shows the resulting spectrum for an assumed thickness $d = 3$ μm. For thicknesses $d \gg c/\omega_{\text{pl}}$ all frequencies below the plasma frequencies would be completely absent in the emission.

The geometry of a laser-induced light string enters our computations in exactly the same way. The eigenmodes have to be computed according to Eq. (11) in the presence of the spatial density profile $n(\mathbf{r})$ of the plasma column. Our problem has well separated length scales; the thermal wavelength of the electrons $\lambda_{\text{th}} \simeq 1$ nm is much smaller than the diameter of the plasma column $R \approx 30$ μm,

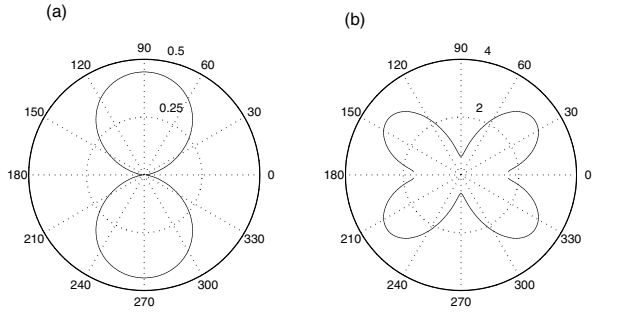

FIG. 2. Mode strength $|u_{\mathbf{q},\sigma}(\mathbf{r}=0)|^2$ for (a) $cq = 1\ \mathrm{ps}^{-1} < \omega_{\mathrm{pl}}$ and (b) $cq \approx 4.5\ \mathrm{ps}^{-1} = 0.8\omega_{\mathrm{pl}}$. The corresponding mode strength in vacuum would be 1.

which is in turn much smaller than typical THz wavelengths λ_{THz}. As far as optical coupling is concerned, the exact form of $n(\mathbf{r})$ is therefore relatively unimportant as long as it is strongly localized, say, at the origin of the $(x-y)$ plane. Following Ref. [20], we have solved for the eigenmodes of Eq. (11) by using a transfer matrix technique. All solutions can be classified by the wave vector $\mathbf{q}$ of an incoming plane wave and its polarization σ distinguishing between TM mode (incident electric field in the plane of incidence) and TE mode (incident electric field perpendicular to electron string).

The mode strength $|\mathbf{u}_{\mathbf{q},\sigma}(\mathbf{r}=0)|^2$ for the TM mode is presented in Fig. 2 for the case of a steplike density profile with a carrier density of $n = 10^{16}\ \mathrm{cm}^{-3}$ over a cylinder with radius $R = 30\ \mu\mathrm{m}$. For frequencies well below the plasma frequency, we find a dipole radiation pattern qualitatively similar to that observed experimentally in Ref. [3]. The main emission is perpendicular to the plasma rod aligned along the horizontal axis of Fig. 2. This emission pattern can be traced back to the increasing suppression of light modes below the plasma frequency as the emission angle deviates more from the normal direction. For frequencies around and above the plasma frequency, the angle dependence drastically changes since this suppression does not exist anymore. For certain frequencies and emission angles resonance effects can be observed which depend on the precise choice of parameters. In the given example, we observe a preferred emission angle around 40°. The mode strength of the TE mode does not strongly depend on the angle of incidence since for any angle the electric field component lies perpendicular to the light string.

In summary, we presented a microscopic theory for the photoluminescence emitted from fs laser-induced plasmas due to electron-ion scattering. The angle dependence of the THz emission for light string induced plasmas was explored using modal analysis, a dipole pattern for emission frequencies below the plasma frequency being found in qualitative agreement with the recent experiment [3]. In contrast, a drastically different angle dependence for emission frequencies above the plasma frequency is predicted. Finally, we note that although our analysis was motivated by studies of THz emission in air [2–4], our results apply more generally, for example, to glasses or electron-hole plasmas in semiconductors.

We thank Marten Richter for valuable discussions. The work is sponsored in Tucson by the U.S. Air Force Office of Scientific Research (AFOSR), under Grant No. AFOSR-F49620-03-1-0194, in Berlin by the Deutsche Forschungsgemeinschaft through the SFB 296, and in Marburg by the Optodynamics Center and the Deutsche Forschungsgemeinschaft.

*Electronic address: hoyer@acms.arizona.edu
†Permanent address: Institut für Theoretische Physik, AG Nichtlineare Optik und Quantenelektronik, Technische Universität Berlin, 10623 Berlin, Germany.

[1] G. Davies and E. Linfield, Phys. World **17**, 37 (2004).
[2] A. Proulx, A. Talebpour, S. Petit, and S. Chin, Opt. Commun. **174**, 305 (2000).
[3] S. Tzortzakis *et al.*, Opt. Lett. **27**, 1944 (2002).
[4] G. Méchain, S. Tzortzakis, B. Prade, M. Franco, A. Mysyrowicz, and B. Leriche, Appl. Phys. B **77**, 707 (2003).
[5] E. Nibbering, P. Curley, G. Grillon, B. Prade, M. Franco, F. Salin, and A. Mysyrowicz, Opt. Lett. **21**, 62 (1996).
[6] S. Tzortzakis, G. Méchain, G. Patalano, M. Franco, B. Prade, and A. Mysyrowicz, Appl. Phys. B **76**, 609 (2003).
[7] J. Yu, D. Mondelain, J. Kasparian, E. Salmon, S. Geffroy, C. Favre, V. Boutou, and J.-P. Wolf, Appl. Opt. **42**, 7117 (2003).
[8] H. Ladouceur, A. Baronavski, D. Lohrmann, P. Grounds, and P. Girardi, Opt. Commun. **189**, 107 (2001).
[9] H. Hamster, A. Sullivan, S. Gordon, W. White, and R. Falcone, Phys. Rev. Lett. **71**, 2725 (1993).
[10] P. Sprangle, J. Peñano, B. Hafizi, and C. Kapetanakos, Phys. Rev. E **69**, 066415 (2004).
[11] T. Bornath, M. Schlanges, P. Hilse, and D. Kremp, Phys. Rev. E **64**, 026414 (2001).
[12] J. Dawson and C. Obermann, Phys. Fluids **5**, 517 (1962).
[13] G. Bekefi, *Radiation Processes in Plasmas* (John Wiley & Sons, Inc., New York, 1966).
[14] D. F. DuBois, in *Lectures in Theoretical Physics*, edited by W. E. Brittin (Gordon and Breach, New York, 1967), Vol. 9C, p. 469.
[15] A. Wierling, T. Millat, and G. Röpke, J. Plasma Phys. **70**, 185 (2004).
[16] C. Cohen-Tannoudji, J. Dupont-Roc, and G. Grynberg, *Photons & Atoms* (Wiley, New York, 1989), 3rd ed.
[17] H. Haug and S. W. Koch, *Quantum Theory of the Optical and Electronic Properties of Semiconductors* (World Scientific Publishing, Singapore, 2004), 4th ed.
[18] H. Wyld and B. Fried, Ann. Phys. (N.Y.) **23**, 374 (1963).
[19] W. Hoyer, M. Kira, and S. Koch, in *Nonequilibrium Physics at Short Time Scales*, edited by K. Morawetz (Springer, Berlin, 2004), pp. 309–335.
[20] A. Helaly, E. Soliman, and A. Megahed, IEE Proc.-Microw. Antennas Propag. **144**, 61 (1997).